Indian Journal of Experimental Biology
Vol. 61, April 2023, pp. 265-275
DOI: 10.56042/ijeb.v61i04.177

Protective effects of grape seed proanthocyanidins on podocytes against injury induced by glucolipotoxicity

Haiyan Li[1†], Tongling Wang[2†], Dandan Liu[3], Yusong Ding[1,2]* & Jinbao Liu[3]*

[1]College of Public Health, Xinjiang Medical University, Urumqi 830011, China

[2]Department of Public Health, Shihezi University School of Medicine, Shihezi 832001, China

[3]Department of Public Health, Xinjiang Second Medical College, Cremayi 834000, Xinjiang, China

Received 10 December 2022; *revised 18 March 2023*

Diabetic nephropathy (DN) is the most common cause of end-stage renal failure, oxidative damage and iron metabolism disorder are related to DN progression, but the exact pathogenesis remains unclear. Grape seed proanthocyanidins extract (GSPE) are one of the most widely distributed polyphenols with antioxidant properties. Here, we evaluated the mechanism by which GSPE alleviates podocyte damage induced by high glucose and palmitic acid (HG/PA). Podocytes were cultured in groups in normal environment; these were based on whether HG/PA and ML385 were present and the GSPE conc. 10, 25 and 50 mg/L. The flow cytometer, immunofluorescence staining, Western blot, quantitative real time-PCR (qRT-PCR), kit method and fluorescence microscope were used, respectively. After HG/PA intervention, the podocyte morphology was destroyed, the survival rate was reduced, the cell apoptosis was increased, and the fluorescence intensity of ROS detection was increased, iron metabolism was disordered. After adding ML385, increased oxidative damage to podocyte, nuclear factor erythroid 2-related factor 2 (Nrf2) and its downstream protein and mRNA expression levels were significantly reduced. However, application of different concentrations of GSPE could reverse these situations. Our findings indicate that GSPE regulates intracellular iron metabolism disorders and reduces the oxidative damage of podocytes possibly through activation of the Nrf2 signaling pathway.

Keywords: Diabetic nephropathy, Iron, NF-E2-Related Factor 2, Oxidative stress

Worldwide, there are about 537 million adults reported to be suffering from diabetes[1]. Despite extensive prevention and treatment measures, 20-40% of diabetic patients will develop different degrees of diabetic nephropathy (DN)[2], primarily manifested as proteinuria, excessive production of mesangial matrix, renal hypertrophy, and fibrosis[3]. DN is the main cause of end-stage renal disease and has become a global health and socioeconomic burden[4-6]. Although there has been some progress in the treatment of DN, the pathogenesis of DN remains unclear. Hence, research on the prevention and treatment of DN is of great significance.

Podocytes are a special type of glomerular cells that are wrapped around capillaries to filter blood and prevent plasma proteins from entering the urine filtrate[7]. Along with mesangial cells, they maintain structural integrity of the glomerulus[8]. Podocyte dysfunction is a major factor in the pathogenesis of DN because it can lead to proteinuria, which is an early symptom of DN[9]. In clinical practice, diabetic patients are characterized by early podocyte loss, in addition to impaired podocyte integrity[10]. Decreased podocyte density can be caused by apoptosis and glomerular basement membrane detachment, which is a predictor of DN progression[11]. Podocyte damage caused by hyperglycemia, including apoptosis, mitochondrial dysfunction, and oxidative stress, is closely related to DN[12-14].

Iron is an essential trace metal for organisms, it catalyzes highly toxic hydroxyl radicals through a Fenton reaction and induces oxidative stress[15]. Previous literature showed the presence of increased iron accumulation in the kidneys of diabetic rats induced by streptozotocin[16]. Renal iron accelerates the progression of DN[17]. Oral iron removers can protect the kidneys of DN rats by reducing oxidative stress, inflammation, and other such conditions, and by promoting iron chelation[18]. Low-iron diet or iron chelating agents can delay the progression of DN[19]. As a new mechanism, iron is believed to regulate the

*Correspondence:
E-Mail 283474978@qq.com (JL); 51603030@qq.com (YD)
†Contributed equally

progression of DN; however, knowledge about how iron promotes the progression of DN is limited.

Grape seed proanthocyanidin extract (GSPE) is a mixture of polyphenols which is composed of catechin, epicatechin, and epicatechin gallate linked mainly through C4–C6 or C4–C8 (B type)[20, 21]. Numerous in vitro and in vivo researches have reported the biological activities of GSPE including anti-inflammatory properties, antioxidant activities, anti-apoptotic and toxicity resistance[22-28]. Our previous studies have shown that grape seed proanthocyanidin extract (GSPE) reduces kidney damage in diabetic rats by activating the Nrf2 signaling pathway[26]. Studies have also revealed that the polyphenol structure of GSPE can exert anti-oxidant properties and antagonize the damage caused by excessive iron, indicating that GSPE can perform these additional functions along with scavenging free radicals and inhibiting lipid peroxidation[29]. GSPE also exhibits great development and application prospects in the prevention and treatment of DN.

In the present study, we explored whether GSPE can regulate iron metabolism disorders, activate the Nrf2 signaling pathway, increase the expression of its downstream antioxidant enzymes, and reduce the oxidative damage of podocytes, thereby playing a significant role in the prevention and early treatment of diabetic nephropathy (DN).

Material and Methods

Chemicals and Reagents

Mouse glomerular podocytes MPC5 were purchased from Shanghai Fuxiang Biological Technology (XF1009, Shanghai, China). GSPE with the content of polyphenols or proanthocyanidins is no less than 95% was obtained from Beijing Soleibao Technology (SP8520, Beijing, China). The total protein assay kit (with standard: BCA method, A045-4), malondialdehyde (MDA) Kit (A003-1), superoxide dismutase (SOD) Kit (A001-3), Glutathione (GSH) Kit (A006-2), and ROS Kit (E004-1-1) were purchased from Nanjing built biological products (Nanjing, China). Divalent metal transporter 1 (DMT1) Kit (JM-12129M1), and Ferroportin 1(FPN1) Kit (JM-11755M1) were purchased from Jiangsu Jingmei Biological Technology (Jiangsu, China). CCK-8 method cell proliferation detection kit (KGA317) and Apoptosis detection kit (KGA101-KGA104) were obtained from Jiangsu KGI Biotechnology (Jiangsu, China). Mouse monoclonal antibody (β-actin,) were obtained from Wuhan Boster Biological Technology. Mouse monoclonal antibody (PCNA) was obtained from Boster (California, USA). Mouse monoclonal antibody (NQO1, HO-1), rabbit monoclonal antibody (Hepcidin, FPN1), rabbit polyclonal antibody (Nrf2), and goat polyclonal antibody (GST) were obtained from Abcam (Cambridge, MA). TRIzol and Transcriptor First Strand cDNA Synthesis Kit were obtained from Invitrogen (Carlsbad, CA, USA) and Roche (Basel, Switzerland). DAPI(C1002), FITC-labeled Goat Anti-Rabbit IgG (H+L) (A0562), pARE-luc(D2112), pRL-TK(D22760), Dual Luciferase Reporter Gene Assay Kit (RG027), Nuclear and Cytoplasmic Protein Extaction Kit (P0027) were obtained from Beyotime Biotechnology (Shanghai, China). Lipofectamine 2000 reagent was obtained from Invitrogen, Carlsbad, CA, USA (11668-019). Lillie Staining Assay kit was obtained from Beijing Soleibao Technology Co., Ltd.(G3320).

Cell culture and treatments

The MPC5 cells were incubated in DMEM supplemented with 10% fetal bovine serum, 100 U/mL penicillin, and 100 μg/mL streptomycin at 37°C in a humidified atmosphere of 5% CO_2. Podocytes were cultured in groups in normal environment; these were based on whether high glucose and palmitate (HG/PA) and ML385 were present and the GSPE concentrations @ 10, 25 and 50 mg/L.

Cell viability assay

The 96-well plate was seeded with $7*10^3$ cells/well of differentiated and mature podocytes, and the cells of each group were intervened according to the experimental protocol. After 24 h, 10 μL of CCK-8 solution was added in the dark, and the cells were cultured in a 37°C incubator for 1 hour. The OD value of each well was detected at 450 nm wavelength.

Cell apoptosis assay

Cells were inoculated into a 6-well plate, and each group of cells was intervened according to the experimental protocol after the cells were adhered to the wall. After 24 h, the cells of each group were digested and collected and washed twice with pre-cooled PBS by centrifugation. These cells were then resuspended in 500 μL of 1*Binding Buffer. The cells were transferred to EP tubes, 5 μL of FITC and 10 μL of PI were added to each tube and mixed gently. They were then incubated in the dark at room temperature

for 10 min and flow cytometry detection was performed.

Cellular ROS analysis

The MPC5 cells were seeded into 6-well plate for culture. After the cells adhered to the wall, each group of cells was intervened according to the experimental protocol. Next, one mL of DCFH-DA probe was added to each group and stained with DCFH-DA at 37℃ for 40 min in the dark. The cell fluorescence was monitored under a fluorescence microscope.

Cellular Iron Metabolism

We assessed the levels of DMT1 and TFR1 in the supernatants of cultured cells using the relevant ELISA according to the manufacturer's instructions. Absorbance was measured at 450 nm using a micro-plate reader. This assay was performed in triplicate.

This was followed by determining the iron content. Each group of cells was intervened according to the experimental protocol. Detection reagents were added according to the instructions of the reagent manufacturer and reacted for 10 min at room temperature. The wave-length of the microplate reader was set to 490 nm, the absorbance of each group was measured, and the total iron level of each group was evaluated.

MDA, SOD, and GSH content assay

The relative content of MDA, SOD and GSH was detected according to the manufacturer's instructions.

Lillie staining

The cellular divalent iron was detected using a Lillie Staining Assay kit following the manufacturer's protocol. Briefly, MPC5 cells were intervened according to the experimental protocol, cells were incubated with Lillie staining solution at 37℃ for 1 h, followed by staining the nucleus with nuclear fast red for 2 min. The images were collected using fluorescence microscope.

Immunofluorescence staining

MPC5 cells were grown in six-well plates to 60% confluence and each group of cells were intervened according to the experimental protocol. The cells were fixed in 4% paraformaldehyde, permeabilized with 0.1% Triton X-100 in PBS for 20 min at room temperature and washed thrice with PBS, then incubated in blocking buffer (5% BSA) for 1 h and then the cells were incubated overnight at 4℃ with the primary antibodies Nrf2 (1:500) and washed thrice with PBS. Add goat anti-rabbit IgG H&L (FITC 1:1,000)) and incubate at room temperature for 2 h and washed thrice with PBS. The nucleus staining was incubated with DAPI for 3 min and washed thrice with PBS. The images were collected using fluorescence microscope.

ARE activity detection

MPC5 cells seeded in 96-well culture plate, grown to 80%-90%, were transfected with pARE-luc and pRL-TK using Lipofectamine 2000 reagent according to the manufacturer's instructions, with a final recombinant vectors concentration of 100 ng. Incubate at 37℃ for 6 h, remove the transfection solution, and each group of cells was intervened according to the experimental protocol. Cells were collected and cell extracts were used to determine luciferase activity according to the manufacturer's instructions. Luciferase activity value is collected using a full-wavelength scanning multi-function reader.

Western blot analysis

The total protein and nuclear protein of each group was extracted separately and their concentration was determined by the BCA method. Protein samples were separated using SDS-PAGE and then transferred onto the PVDF membranes. The membranes were blocked at room temperature for 2 h with 5% skim milk and incubated overnight at 4℃ with the primary antibodies, β-actin (1:500), PCNA (1:500), Hepcidin (1:1,000), FPN1 (1:1,000), Nrf2 (1:1,000), GST (1:3,000), HO-1 (1:1,000), and NQO1 (1:1,000). The membranes were washed thrice with PBST (TBS and 20% Tween 20) for 10 min each time, incubated with the secondary antibodies at room temperature for 2 h, and washed thrice with PBST. Finally, the membranes were soaked with enhanced chemiluminescence reagent and exposed to X-ray film. Image Lab 4.1 was used to detect and analyze the results. All Western blot analyses were performed in triplicate.

Real-time PCR

Total RNA was isolated from MPC5 cells using TRIzol according to the manufacturer's instructions. cDNA synthesis was then executed by using the Transcriptor First Strand cDNA Synthesis Kit. The primer sequences for real-time PCR analysis are shown in Table 1. The data were analyzed using the $2^{-\triangle\triangle Ct}$ method. The primer sequences for the real-time PCR analysis are shown in Table 1.

Statistical analysis

Statistical analyses were performed using SPSS 20.0 and GraphPad Prism 5.0 software. The experimental data of each group followed a normal

Table 1 — Primer sequences for quantitative real-time polymerase chain reaction

Name	Primer	Sequence	Size
Mus GAPDH	Forward	ATGGGTGTGAACCACGAGA	
	Reverse	CAGGGATGATGTTCTGGGCA	229
Mus Hepcidin	Forward	CTGTCTCCTGCTTCTCCTCC	
	Reverse	TGGGGAAGTTGGTGTCTCTC	161
Mus FPN1	Forward	GTGGAGACTACTTCCGTGCT	
	Reverse	GCCCCAGAAGATATGTCGGA	148
Mus Nrf2	loop primer	CAGTGCTCCTATGCGTGAA	
	F primer	GCGGCTTGAATGTTTGTCT	109
Mus HO-1	loop primer	CCTCACTGGCAGGAAATCA	
	F primer	TCGGGAAGGTAAAAAAAGC	217
Mus NQO1	Forward	GGCTGGTTTGAGAGAGTGCT	
	Reverse	GGAAGCCACAGAAACGCAG	205
Mus GST	Forward	GCTCTTTGGGGCTTTATGGG	
	Reverse	GCAGGGTCTCAAAAGGCTTC	177

[FPN1: Ferroportin 1; Nrf2: nuclear factor erythroid 2-related factor 2; HO-1: Heme Oxygenase 1; NQO1: NAD(P)H quinone oxidoreductase 1; GST: glutathione S-transferase]

distribution and are presented as the mean ± standard deviation. Comparison of differences in each group was performed through analysis of variance. The correlation analysis of the data was conducted using the Spearman correlation coefficient. P <0.05 indicated statistical significance.

Results

Effect of GSPE on podocyte morphology, viability, ROS, Nrf2 and iron metabolism levels

To obtain the optimal concentration through preliminary experiments, 10, 25 and 50 mg/L were selected as the concentrations of GSPE. The cells were co-cultured with above concentrations of GSPE, and it was found that after adding GSPE, the cell morphology did not change significantly compared with the control group (Fig. 1A). Detection of cell viability with CCK8 showed that there was no statistical difference in cell

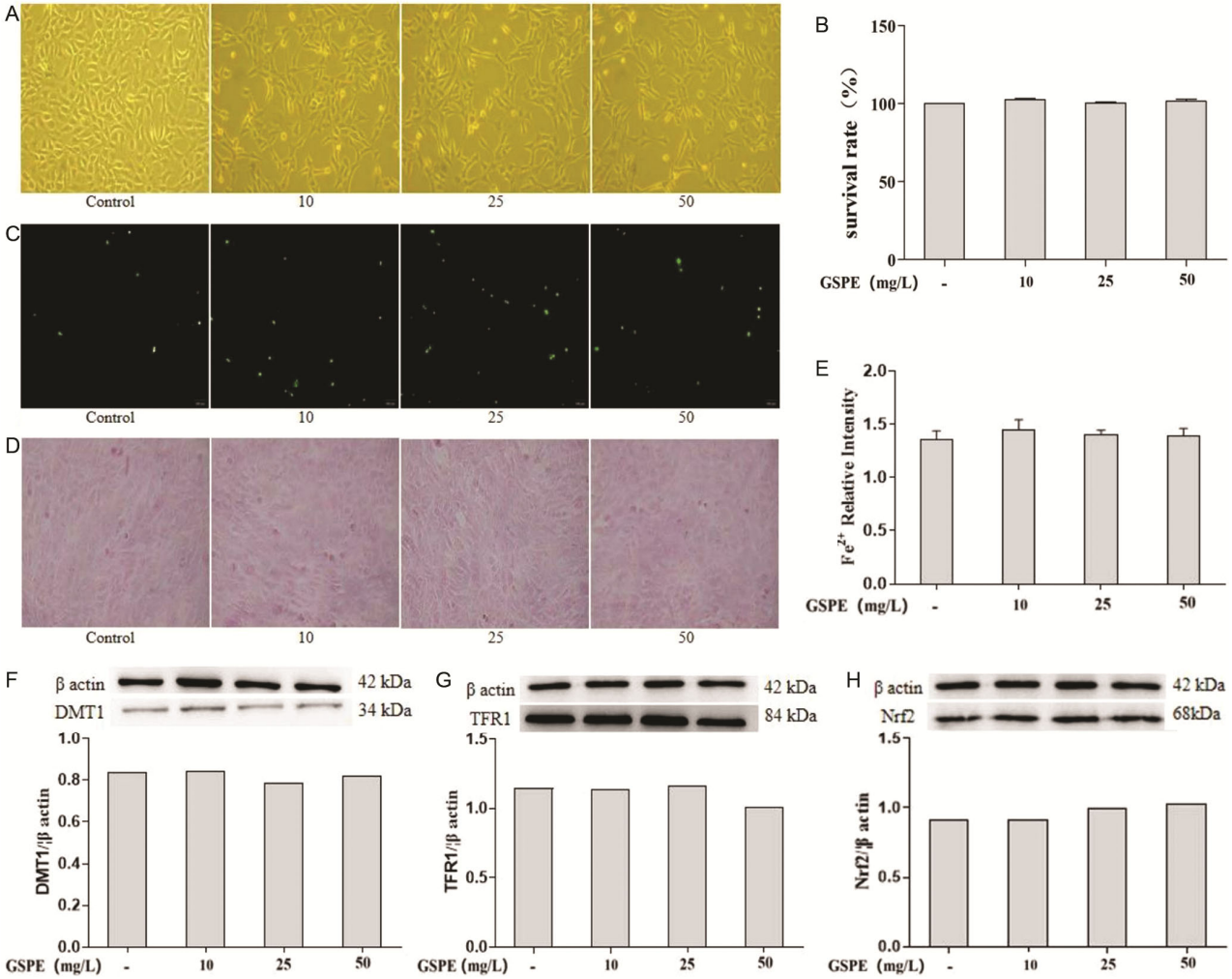

Fig. 1 — Effect of grape seed proanthocyanidins extract (GSPE) on (A) morphology and structure; (B) survival rate; (C) ROS; (D) divalent iron (blue); (E) relative intensity; (F) DMT1; (G) TFR1; and (H) Nrf2 (H) of podocytes. Control, Control group; GSPE treatment groups @ 10, 25 and 50 mg/L. [Original magnification of (A, C & D) 400X]

viability between the 10, 25 and 50 mg/L GSPE groups compared with the control group (P >0.05, Fig. 1B). The fluorescence intensity of ROS was observed under a fluorescence microscope, and it was found that after adding GSPE, the ROS level was not changed (Fig. 1C). No obvious blue spots were seen in each group, indicating that there was no accumulation of ferrous ions in the cells (Fig. 1 D-E). There is no difference in the expression of DMT1, TFR1 and Nrf2 (Fig. 1 F-H). The above results indicate that within this dose range, GSPE is safe and harmless to podocytes, the use of GSPE in normal podocytes did not cause iron metabolism disorders and oxidative stress.

GSPE mitigates glucolipotoxicity-induced injury of podocytes

To study the role of GSPE in podocyte injury induced by glycolipid toxicity, an *in vitro* injury model induced by HG/PA was established while administering different concentrations of GSPE. Observed under a light microscope, the cell morphology of the control group was spindle-shaped and normal. After the HG/PA intervention, the number of cell attachments decreased and the cells shrank, indicating cell damage. After the intervention of different concentrations of GSPE, compared with the injury group, the number of adherent cells increased, the cell shrinkage was improved, and some cells returned to normal (Fig. 2A). After the HG/PA intervention, the survival rate of podocytes decreased and the rate of apoptosis increased (Fig. 2 B-D). After assessing the level of ROS, it was found that the fluorescence intensity under the fluorescence microscope was increased (Fig. 2 E-F). After co-cultivation with different doses of GSPE, the survival rate of cells increased and the rate of apoptosis decreased, ROS levels showed that the fluorescence intensity under the fluorescence microscope gradually decreased (P <0.05, Fig. 2 B-F).

GSPE regulates iron metabolism disorders in podocytes induced by HG/PA

DMT1 and TFR1 are commonly used indicators reflecting the level of cellular iron metabolism. After HG/PA stimulation, the levels of DMT1, TFR1, total iron, and intracellular iron in the injury group were higher than those in the control group (P <0.05, Fig. 3 A-E). The expression of Hepcidin, FPN1 protein, and mRNA in the injury group was significantly lower than that in the control group (P <0.05, Fig. 3 F-I). However, after adding different doses of GSPE, the above situation was reversed (P <0.05, Fig. 3). This shows that GSPE regulates the iron metabolism disorder of podocytes induced by HG/PA.

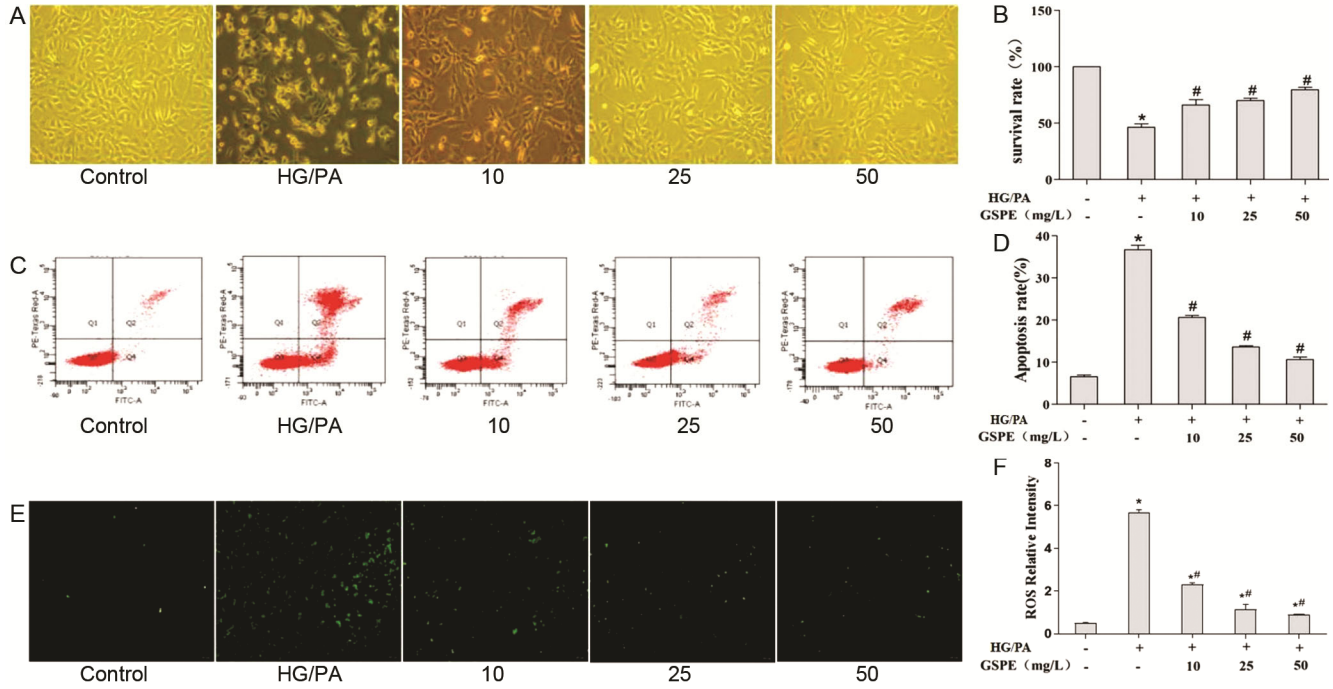

Fig. 2 — Effects of glucolipotoxicity and GSPE on (A) morphology and structure; (B) survival rate; (C & D) apoptosis; and (E & F) ROS of podocytes. [Control, Control group; HG/PA, high glucose and palmitic acid group; GSPE treatment groups @ 10, 25 and 50 mg/L. Original magnification of (A) 400X]

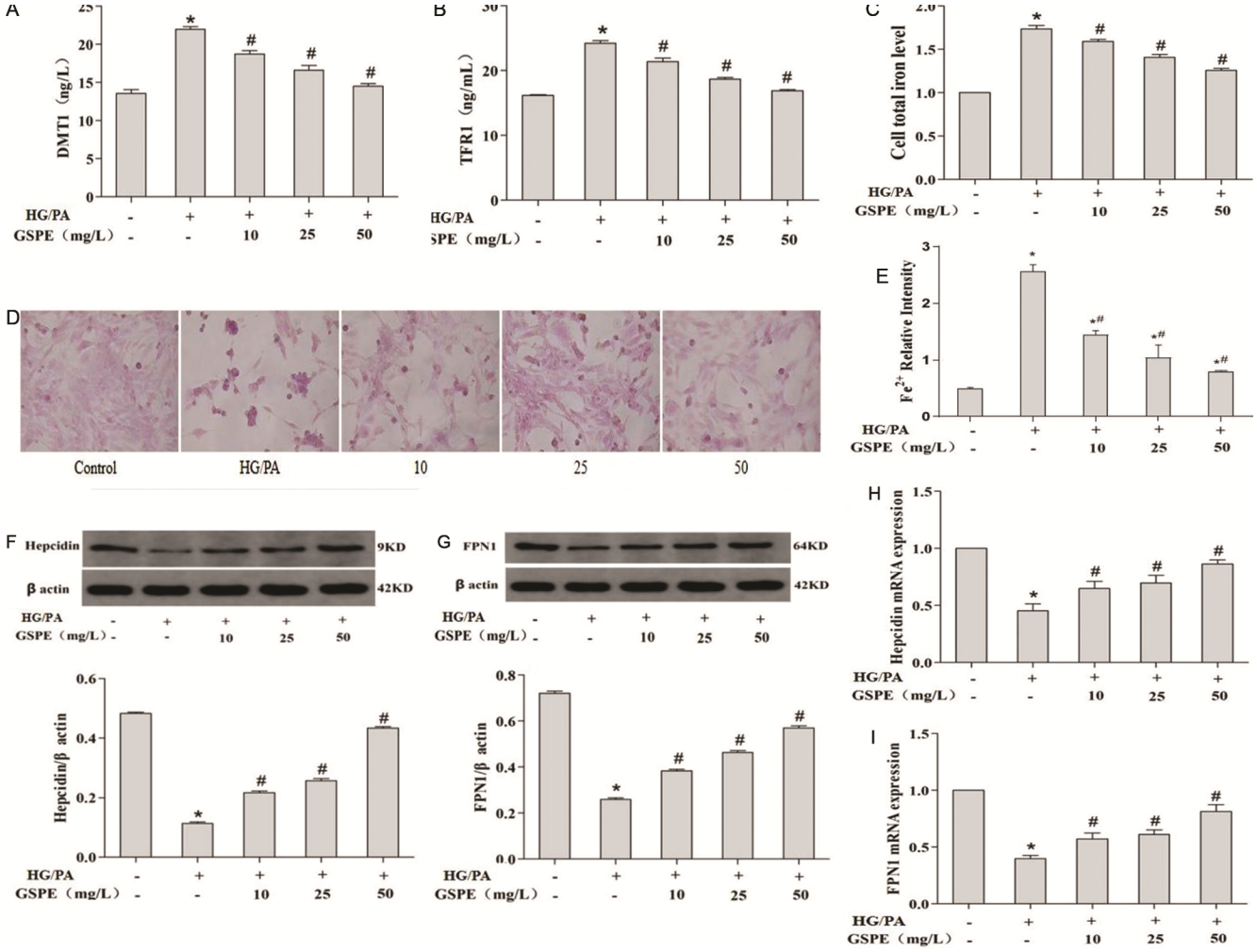

Fig. 3 — Effects of HG/PA and GSPE on cell (A) DMTI; (B) TFR1; (C) total iron levels; (D & E) divalent iron (blue); and (F-I) Hepcidin, FPN1 protein and mRNA levels. [HG/PA, high glucose and palmitic acid group; GSPE, Grape seed proanthocyanidin extract; GSPE treatment groups @ 10, 25 and 50 mg/L. Values are presented as mean ± standard deviation (n=3). **P* <0.05 *vs*. the control group; #*P* <0.05 *vs*. the HG/PA group. Original magnification of (D) 400X]

GSPE reduces oxidative damage caused by HG/PA to podocytes by activating Nrf2

Intervention was performed by adding or not adding ML385 to inhibit the expression of Nrf2, while using HG/PA to cause oxidative damage to podocytes. Different doses of GSPE were applied to activate the Nrf2 signaling pathway and detect oxidation- Anti-oxidant damage index. Compared with the control group, it was found that the SOD and GSH content in the injury group were significantly reduced, and the MDA content was significantly increased. After adding different doses of GSPE, compared with the injury group, the SOD and GSH content gradually increased, and the MDA content gradually decreased (*P* <0.05, Table 2). After pretreatment with Nrf2 inhibitor ML385, the treatment continued with HG/PA and GSPE. The results showed that the SOD and GSH content of the injury group was significantly reduced compared with the control group, and the MDA content further increased. However, after the combined intervention of 50 mg/L GSPE in the injury group, the SOD and GSH content increased compared with the injury group, while the MDA content decreased (*P* <0.05, Table 2). It is suggested that when the Nrf2 signal pathway is inhibited, the antioxidant effect of GSPE is weakened.

Iron metabolism is related to oxidative damage

The results of the correlation analysis of oxidation-antioxidant indexes and iron metabolism indexes showed that SOD and GSH were negatively correlated with DMT1, TFR1, and total iron, and that MDA was positively correlated with DMT1, TFR1, and molten iron (*P* <0.05, Table 3), suggesting that iron metabolism is related to oxidative damage.

Table 2 — Inhibition or activation of Nrf2 affects podocyte oxidative damage induced by HG/PA

	SOD	GSH	MDA
Control	23.61±0.54	34.69±0.37	9.07±0.62
HG/PA	13.68±0.48*	22.61±0.87*	17.28±0.28*
HG/PA+10 mg/L GSPE	18.55±0.73#	27.32±0.91#	15.56±0.40#
HG/PA+25 mg/L GSPE	20.53±0.73#	32.52±1.63#	14.17±0.52#
HG/PA+50 mg/L GSPE	21.37±0.39#	33.46±0.97#	9.86±0.50#
ML385	12.49±1.21	13.17±0.30	16.46±0.78
ML385+HG/PA	7.72±0.75*	7.13±0.81*	20.30±0.94*
ML385+HG/PA+10 mg/L GSPE	8.14±0.43	6.17±0.76	17.68±0.56#
ML385+HG/PA+25 mg/L GSPE	9.48±1.07#	7.91±0.35	15.39±0.86#
ML385+HG/PA+50 mg/L GSPE	9.69±0.97#	9.59±0.83#	14.20±0.58#
F	117.39	558.33	87.99
P	＜0.001	＜0.001	＜0.001

[Control, Control group; HG/PA, high glucose and palmitic acid; ML385: ML385 treatment group. Values are presented as mean ± SD (n=3). *P <0.05 *vs*. the control group before and after Nrf2 inhibition, respectively; # P <0.05 *vs*. the injury group before and after Nrf2 inhibition, respectively]

Table 3 — Correlation analysis of oxidation-antioxidant indexes and iron metabolism indexes

	SOD	GSH	MDA	DMT1	TFR1	Total iron
SOD	-	0.943*	–0.878*	–0.957*	–0.949*	–0.928*
GSH	0.943*	-	–0.886*	–0.948*	–0.966*	–0.959*
MDA	–0.878*	–0.886*	-	0.938*	0.937*	0.952*
DMT1	–0.957*	–0.948*	0.938*	-	0.950*	0.957*
TFR1	–0.949*	–0.966*	0.937*	0.950*	-	0.967*
Total iron	–0.928*	–0.959*	0.952*	0.957*	0.967*	-

[DMT1, Divalent metal transporter; GSH, Glutathione; MDA, malondialdehyde; 1; SOD, superoxide dismutase; TFR1, Ferroportin 1. *Refers to P <0.05)]

Effect of GSPE on ARE levels and Nrf2, HO-1, GST, NQO1 protein and mRNA expression in HG/PA-induced podocyte injury

To further confirm that GSPE promoted HG/PA induced distribution of Nrf2 in podocyte, immunofluorescence staining was performed to investigate the distribution of Nrf2. The images indicated that GSPE could significantly increase Nrf2 staining (green) in the nucleus, suggesting that GSPE promote the nuclear translocation of Nrf2 (P <0.05, Fig. 4 A and B), and the results were consistent western blot (P <0.05, Fig. 4C). The results of the luciferase analysis revealed that GSPE significantly increased ARE-mediated luciferase activity in a concentration-dependent manner (P <0.05, Fig. 4D). Compared with the control group, the protein and mRNA expression levels of total Nrf2, HO-1, NQO1, and GST in the injury group were significantly reduced, after adding different doses of GSPE, compared with the injury group, the Nrf2, HO-1, protein, and mRNA expression of NQO1 and GST increased significantly (P <0.05, Fig. 4 E-L). Using ML385 to inhibit the expression of Nrf2, and after the co-intervention with HG/PA and GSPE, the protein and mRNA expression levels of Nrf2, HO-1, NQO1, and GST in the ML385+HG/PA group were lower than those of ML385 (P <0.05). After adding 50 mg/L of GSPE to the ML385+HG/PA group, the protein and mRNA expression of Nrf2, HO-1, NQO1, and GST increased, and there was a statistical difference (P <0.05, Fig. 4 E-L). It is suggested that GSPE can increase the expression of Nrf2 and its downstream proteins and mRNA in podocytes under HG/PA conditions, and activate Nrf2 into the nucleus.

Discussion

Although the pathogenesis of DN is not completely clear, many studies have pointed out that oxidative stress is involved in the occurrence and development of DN[26, 30-31]. When there are excessive iron ions in the body, the excessive iron ions will become a catalyst for oxidative damage in the body, generating a large amount of hydroxyl free radicals and aggravating the damage caused by oxidative stress[32]. Studies have pointed out that GSPE can improve the symptoms of DN by regulating oxidative stress[26]. In this study, GSPE was used to interfere with HG/PA-induced podocyte damage. The detection of related indicators found that HG/PA can inhibit the expression of Nrf2 and its related proteins, increase DMT1 and TFR1 levels, reduce FPN1 and Hepcidin protein and gene expression, cause ROS accumulation, reduce SOD and GSH activity, increase MDA content, and increase cell apoptosis. GSPE can reverse the damage caused by HG/PA to podocytes. These results indicate that GSPE regulates iron metabolism disorders and increases antioxidant capacity by activating the Nrf2 signaling pathway, thereby antagonizing the damage caused by HG/PA to podocytes.

In the early stage of DN, podocyte apoptosis is the key target of glomerular damage, it precedes the development of DN and worsens the patient's renal function. Therefore, inhibiting podocyte apoptosis caused by HG/PA is one of the important measures to prevent and treat DN[33]. Consistent with previous findings, in this study, cell morphology changed under HG/PA conditions, survival rate decreased, and podocyte apoptosis levels increased[34]. After intervention with GSPE, this result was reversed,

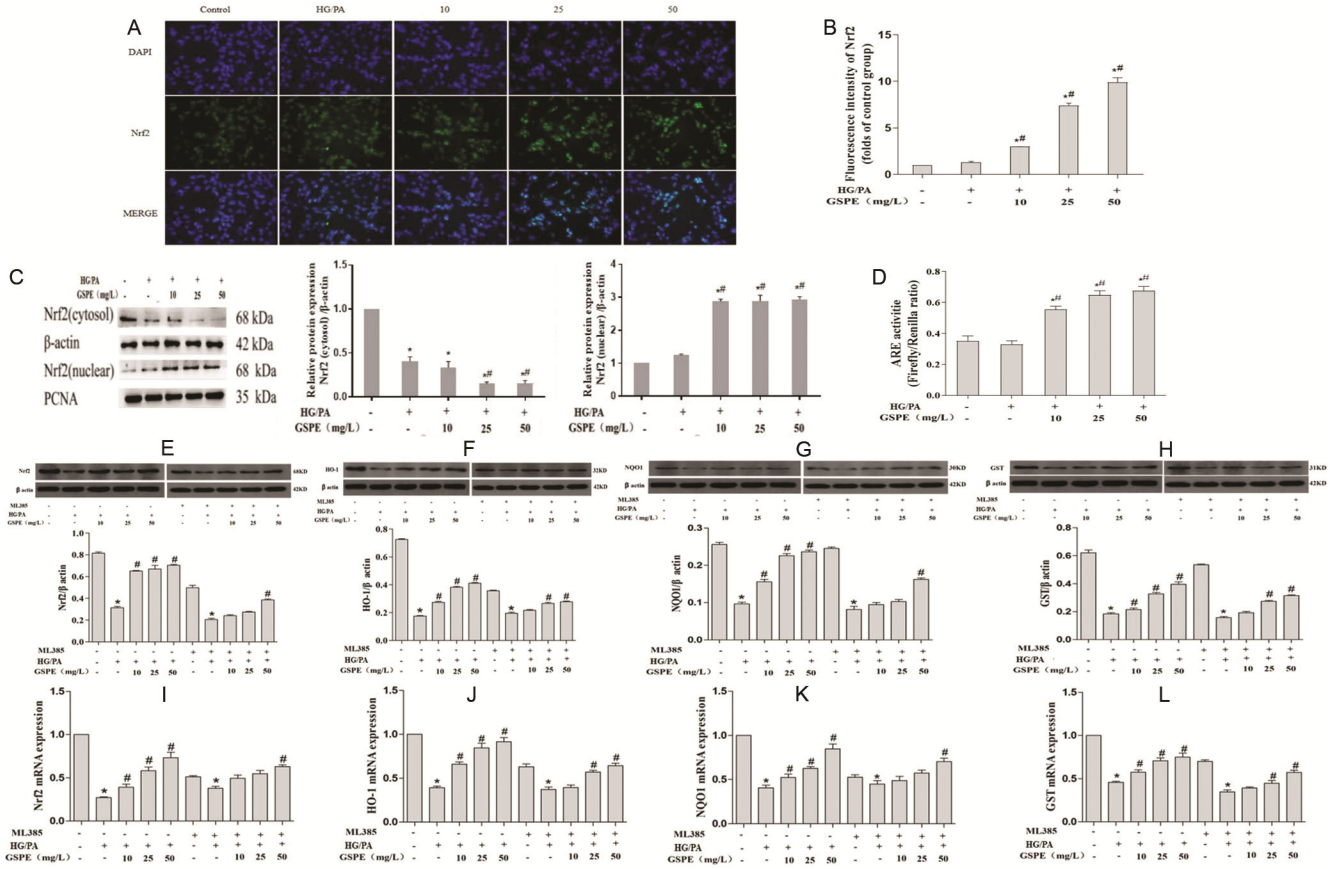

Fig. 4 — GSPE treatment (A & B) activates Nrf2 into the nucleus through Immunofluorescence; (C) increases expression level of nuclear Nrf2 protein and decrease the expression level of cytosol Nrf2 protein; (D) reverses the decreased ARE levels in the injury group caused by HG/PA; (E-L) reverses the decreased protein and mRNA expression levels of Nrf2, HO-1, NQO1, GST in the injury group caused by HG/PA, and the use of ML385 to inhibit Nrf2 significantly inhibits the protein and mRNA of Nrf2, HO-1, NQO1, and GST Expression level, but GSPE could reverse this situation. [HG/PA, high glucose and palmitic acid group; GSPE treatment groups @ 10, 25 and 50 mg/L. Values are presented as mean ± standard deviation (n=3). **P* <0.05 *vs*. the control group before and after Nrf2 inhibition, respectively; $^{\#}P$ <0.05 *vs*. the injury group before and after Nrf2 inhibition, respectively, Original magnification of (A) 400X]

suggesting that GSPE could antagonize cell apoptosis caused by glycolipid disorders.

Iron is one of the essential micronutrients of the human body that is primarily responsible for the transport of oxygen, it participates in the formation of highly active free radicals, which can induce the oxidative modification of various molecules[35-36]. Iron-mediated oxidative stress has been considered to be an important cause of chronic kidney injury[37]. Cellular iron levels are dependent on iron import, storage, utilization and export, which are mainly regulated by the iron response element-iron regulatory protein system. In our research, the results of correlation analysis between iron metabolism indicators and oxidative damage indicators show the existence of a correlation between these indicators. It has been reported that the level of hepcidin is decreased under conditions of high glucose stimulation, which is consistent with the results of the present study[38]. Lower levels of hepcidin may contribute to iron overload by preventing iron exportation or increasing iron intake[39-40], mainly by upregulating the expression of TFR1 and DMT1, resulting in iron accumulation within cells. Our study also show that under HG/PA conditions, the iron export protein FPN1 decreases, which directly leads to the accumulation of intracellular iron, and which is consistent with our measured intracellular total iron levels and the results of intracellular bivalent iron staining. When iron is overloaded in cells, it will destroy the redox homeostasis and catalyze the generation of ROS, leading to oxidative stress[38].

According to reports, polyphenols, curcumin and quercetin can regulate the level of iron metabolism-related proteins[41]. This study found that GSPE as one

of the most widely distributed flavonoids in the plant kingdom can regulate iron homeostasis caused by HG/PA in podocytes and maintain normal cellular iron metabolism. GSPE can decrease the levels of DMT1 and TFR1, reduce iron input, at the same time, increase the expression of FPN1 and Hepcidin, accelerate the transport of iron out of the cell, finally, reduce the iron level of the cell[42]. The use of GSPE to regulate iron metabolism is expected to improve DN.

An increasing number of studies show that glucose-induced oxidative stress has become a key pathogenic factor of DN[43]. In line with the results of the previous studies, our results reveal that GSPE can reverse the changes in podocyte ROS, SOD, GSH, MDA, and other indicators induced by HG/PA. ROS is key in inducing oxidative damage. The MDA content reflects the degree of cell lipid peroxidation damage, while SOD and GSH indirectly reflect the body's ability to scavenge oxygen free radicals. This result shows that under certain conditions, endogenous antioxidants cannot neutralize oxidative stress. At this time, exogenous antioxidants are needed to enhance the antioxidant system[44]. This is consistent with our previous study of using GSPE to protect kidney damage in diabetic rats[26]. This shows that GSPE has strong antioxidant properties, can reduce the oxidative damage of the podocytes, and protect the podocytes.

The Fenton reaction produces ROS due to iron overload, excessive ROS are also produced in a high-sugar state, which consumes the antioxidant proteins that are increased by the body's own Nrf2/ARE pathway activation, and weakens the body's ability to resist oxidative stress[45]. Basic research has proven that Nrf2 has a protective effect on DN, it may be that hyperactivation of nrf2 can increase GSH production and prevent the progression of early renal ischemia-reperfusion injury[46-47]. Therefore, we speculate that the mechanism by which GSPE can antagonize HG/PA-induced podocyte oxidative damage may be related to the activation of the Nrf2 signaling pathway. The results of this experiment show that after GSPE activates Nrf2, it significantly improves the oxidative damaged state of podocytes. The inhibitory effect of Nrf2 inhibitor ML385 on Nrf2 reduces the protective effect of GSPE-mediated against HG/PA-induced podocyte damage. In addition, the degree of oxidative damage is significantly enhanced. Thus, it is speculated that the antioxidant effect of GSPE may be related to the activation of the Nrf2 signaling pathway.

To clarify the mechanism of GSPE's protective effect on podocytes in a HG/PA environment, we used immunofluorescence to detect the nuclear transfer of Nrf2, western blot to detect the expression of nuclear Nrf2 and cytosol Nrf2 protein, and tested the activity of ARE. The results showed that GSPE was found to promote the nuclear translocation of Nrf2 and increase the level of ARE, thereby activating the Nrf2/ARE pathway and its downstream antioxidant proteins in podocytes induced by HG/PA. Next, the expression of Nrf2 and its downstream genes and proteins were analyzed, and it was found that GSPE could improve the protein and mRNA expression of Nrf2, HO-1, NQO1, and GST in podocytes of the injured group. This is consistent with our previous study, which showed that the expression of Nrf2, NQO1, and HO-1 in the kidneys of diabetic rats was increased after GSPE administration[26]. However, GSPE did not cause changes in Nrf2 expression and in that of related proteins in normal podocytes, further confirming that Nrf2 is activated under oxidative stress. In the present study, it was observed that the expression of total Nrf2 and its downstream genes in podocytes decreased after HG/PA stimulation, which is similar to the results of Ali et al[48]. Keap1 is inactivated, leading to the stabilization and accumulation of Nrf2 after HG/PA stimulation, which is consistent with the detection of Nrf2 accumulation in the nucleus and a decrease in cytoplasmic Nrf2, while excessive oxidative stress consumes a large amount of Nrf2, disrupting homeostasis[49]; therefore, total Nrf2 is reduced. Even with inducers, the signal that promotes Nrf2 synthesis is also eventually attenuated with continued challenge, and although the mechanism of this inhibitory response is unclear[50], it may be one reason for the reduction of total Nrf2 and its related proteins after HG/PA stimulation.

It has been reported that ML385 binds to the Neh1 DNA-binding domain of Nrf2, blocks the binding of the Nrf2-MAFG complex to the ARE sequence in the promoter, and reduces the transcriptional activity of Nrf2[50]. To further clarify the activation effect of GSPE on Nrf2, this study included ML385 in advance to pretreat each group and used different doses of GSPE to interfere with the cells under HG/PA conditions. Compared with the inhibited control group, the inhibition of the protein and mRNA

expressions of Nrf2, HO-1, NQO1, and GST in the injured group were lower. After co-intervention with 50 mg/L GSPE, the protein and mRNA expression levels of Nrf2, HO-1, NQO1, and GST in the GSPE group were higher than those in the inhibited injury group, and as the dose of GSPE increased, the inhibitory effect of ML385 on Nrf2 signaling pathway weakened, suggesting that GSPE is a powerful activator of Nrf2 signaling pathway.

Conclusion

Based on the results of our high glucose\palmitic acid (HG/PA) podocyte injury model, our above study on the antioxidative damage effect of grape seed proanthocyanidins extract (GSPE) we can conclude that GSPE can increase the survival rate of podocytes under HG/PA conditions, reduce ROS accumulation, and reduce apoptosis. In addition, it can regulate the iron metabolism disorder in the podocytes under HG/PA conditions, reduce iron accumulation, and reduce oxidative damage. Its mechanism may be through activating the Nrf2 signaling pathway, enhancing the cell's antioxidant capacity, reducing intracellular iron deposition, regulating the iron metabolism disorder,and then improving podocyte damage caused by HG/PA.

Acknowledgment

Authors thand the Postdoctoral Science Foundation of China (NO.2017M613310XB) for funding this work.

Conflict of interest

Authors declare no competing interests.

References

1 Sun H, Saeedi P, Karuranga S, Pinkepank M, Ogurtsova K, Duncan BB, Stein C, Basit A, Chan JCN, Mbanya JC, Pavkov ME, Ramachandaran A, Wild SH, James S, Herman WH, Zhang P, Bommer C, Kuo S, Boyko EJ & Magliano DJ, IDF Diabetes Atlas: Global, regional and country-level diabetes prevalence estimates for 2021 and projections for 2045. *Diabetes Res Clin Pract*, 183 (2022) 109119.

2 Zou LX & Sun L. Global diabetic kidney disease research from 2000 to 2017: A bibliometric analysis. *Medicine* (*Baltimore*), 98 (2019) e14394.

3 Feliers D, Lee HJ & Kasinath BS, Hydrogen Sulfide in Renal Physiology and Disease. *Antioxid Redox Signal*, 25 (2019) 720.

4 Mistry KN, Dabhi BK & Joshi BB, Evaluation of oxidative stress biomarkers and inflammation in pathogenesis of diabetes and diabetic nephropathy. *Indian J Biochem Biophys*, 57 (2020) 45.

5 Johansen KL, Chertow GM, Foley RN, Gilbertson DT, Herzog CA & Ishani A, US Renal Data System 2020 Annual Data Report: Epidemiology of Kidney Disease in the United States. *Am J Kidney Dis*, 77 (2021) A7.

6 GBD Chronic Kidney Disease Collaboration, Global, regional, and national burden of chronic kidney disease, 1990-2017: a systematic analysis for the Global Burden of Disease Study 2017. *Lancet*, 395 (2020) 709.

7 Podgórski P, Konieczny A, Lis Ł, Witkiewicz W & Hruby Z. Glomerular podocytes in diabetic renal disease. *Adv Clin Exp Med*, 28 (2019) 1711.

8 Yadav N, Sharma S, Sharma KP, Pandey A, Pareek P & Sharma S, Protective role of diet supplements Spirulina and Tamarind fruit pulp on kidney in sodium fluoride exposed Swiss albino mice: Histological and biochemical indices. *Indian J Exp Biol*, 54 (2016) 44.

9 Hou Y, Lin S, Qiu J, Sun W, Dong M & Xiang Y, NLRP3 inflammasome negatively regulates podocyte autophagy in diabetic nephropathy. *Biochem Biophys Res Commun*, 521 (2020) 791.

10 Diez-Sampedro A, Lenz O & Fornoni A, Podocytopathy in diabetes: a metabolic and endocrine disorder. *Am J Kidney Dis*, 58 (2011) 637.

11 Weil EJ, Lemley KV, Mason CC, Yee B, Jones LI & Blouch K, Podocyte detachment and reduced glomerular capillary endothelial fenestration promote kidney disease in type 2 diabetic nephropathy. *Kidney Int*, 82 (2012) 1010.

12 Wang L & Li H. MiR-770-5p facilitates podocyte apoptosis and inflammation in diabetic nephropathy by targeting TIMP3. *Biosci Rep*, 40 (2020) BSR20193653.

13 Wang S, Yang Y, He X, Yang L, Wang J & Xia S, Cdk5-Mediated Phosphorylation of Sirt1 Contributes to Podocyte Mitochondrial Dysfunction in Diabetic Nephropathy. *Antioxid Redox Signal*, 34 (2021) 171.

14 Liang Y, Liu H, Fang Y, Lin P, Lu Z & Zhang P, Salvianolate ameliorates oxidative stress and podocyte injury through modulation of NOX4 activity in db/db mice. *J Cell Mol Med*, 25 (2021) 1012.

15 Dixon SJ, Lemberg KM, Lamprecht MR, Skouta R, Zaitsev EM & Gleason CE, Ferroptosis: an iron-dependent form of nonapoptotic cell death. *Cell*, 149 (2012) 1060.

16 Dominguez JH, Liu Y & Kelly KJ, Renal iron overload in rats with diabetic nephropathy. *Physiol Rep*, 3 (2015) e12654.

17 Chaudhary K, Chilakala A, Ananth S, Mandala A, Veeranan-Karmegam R & Powell FL, Renal iron accelerates the progression of diabetic nephropathy in the HFE gene knockout mouse model of iron overload. *Am J Physiol Renal Physiol*, 317 (2019) F512.

18 Zou C, Liu X, Liu R, Wang M, Sui M & Mu S, Effect of the oral iron chelator deferiprone in diabetic nephropathy rats. *J Diabetes*, 9 (2017) 332.

19 Ikeda Y, Enomoto H, Tajima S, Izawa-Ishizawa Y, Kihira Y & Ishizawa K, Dietary iron restriction inhibits progression of diabetic nephropathy in db/db mice. *Am J Physiol Renal Physiol*, 304 (2013) F1028.

20 Yu H, Chen B & Ren Q, Baicalin relieves hypoxia-aroused H9c2 cell apoptosis by activating Nrf2/HO-1-mediated HIF1alpha/BNIP3 pathway. *Artif Cells Nanomed Biotechnol*, 47 (2019) 3657.

21 David JA, Rifkin WJ, Rabbani PS & Ceradini DJ, The Nrf2/Keap1/ARE Pathway and Oxidative Stress as a

Therapeutic Target in Type II Diabetes Mellitus. *J Diabetes Res*, (2017) 4826724.

22 Luo L, Bai R, Zhao Y, Li J, Wei Z & Wang F, Protective Effect of Grape Seed Procyanidins against H2O2-Induced Oxidative Stress in PC-12 Neuroblastoma Cells: Structure-Activity Relationships. *J Food Sci*, 83 (2018) 2622.

23 Silva, J. M. R. D. , Rigaud, J. , Cheynier, V. , Cheminat, A. & Moutonnet, M, Procyanidin dimers and trimers from grape seeds. *Phytochemistry*, 30 (1991) 1259.

24 Liu M, Yun P, Hu Y, Yang J, Khadka RB & Peng X, Effects of Grape Seed Proanthocyanidin Extract on Obesity. *Obes Facts*, 13 (2020) 279.

25 Hu Y, Wei M, Niu Q, Ma R, Li Y & Wang X, Grape seed proanthocyanidin extract alleviates arsenic-induced lung damage through NF-κB signaling. *Exp Biol Med (Maywood)*, 244 (2019) 213.

26 Ding Y, Li H, Li Y, Liu D, Zhang L & Wang T, Protective Effects of Grape Seed Proanthocyanidins on the Kidneys of Diabetic Rats through the Nrf2 Signalling Pathway. *Evid Based Complement Alternat Med*, (2020) 5205903.

27 Chang X, Tian M, Zhang Q, Liu F, Gao J & Li S, Grape seed proanthocyanidin extract ameliorates cisplatin-induced testicular apoptosis via PI3K/Akt/mTOR and endoplasmic reticulum stress pathways in rats. *J Food Biochem*, 21 (2021) e13825.

28 Mohammed ET & Safwat GM, Grape Seed Proanthocyanidin Extract Mitigates Titanium Dioxide Nanoparticle (TiO2-NPs)-Induced Hepatotoxicity Through TLR-4/NF-κB Signaling Pathway. *Biol Trace Elem Res*, 196 (2020) 579.

29 Zhou H, Yin C, Zhang Z, Tang H, Shen W & Zha X, Proanthocyanidin promotes functional recovery of spinal cord injury via inhibiting ferroptosis. *J Chem Neuroanat*, 107 (2020) 101807.

30 Yaribeygi H, Atkin SL & Sahebkar A, A review of the molecular mechanisms of hyperglycemia-induced free radical generation leading to oxidative stress. *J Cell Physiol*, 234 (2019) 1300.

31 Bhatti R, Sharma S, Singh J, Singh A & Ishar MPS, Effect of Aegle marmelos (L.) Correa on alloxan induced early stage diabetic nephropathy in rats. *Indian J Exp Biol*, 51 (2013) 464.

32 Hirschhorn T & Stockwell BR, The development of the concept of ferroptosis. *Free Radic Biol Med*, 133 (20190) 130.

33 Zhao K, Li Y, Wang Z, Han N & Wang Y, Carnosine Protects Mouse Podocytes from High Glucose Induced Apoptosis through PI3K/AKT and Nrf2 Pathways. *Biomed Res Int*, (2019) 4348973.

34 Wang X, Liu Q, Kong D, Long Z, Guo Y & Wang S, Down-regulation of SETD6 protects podocyte against high glucose and palmitic acid-induced apoptosis, and mitochondrial dysfunction via activating Nrf2-Keap1 signaling pathway in diabetic nephropathy. *J Mol Histol*, 51 (2020) 549.

35 Yang WS & Stockwell BR, Ferroptosis: Death by Lipid Peroxidation. *Trends Cell Biol*, 26 (2016) 165.

36 Muckenthaler MU, Rivella S, Hentze MW & Galy B, A Red Carpet for Iron Metabolism. *Cell*, 168 (2014) 344.

37 van Swelm RPL, Wetzels JFM & Swinkels DW, The multifaceted role of iron in renal health and disease. *Nat Rev Nephrol*, 16 (2020) 77.

38 Mao X, Chen H, Tang J, Wang L & Shu T, Hepcidin links gluco-toxicity to pancreatic beta cell dysfunction by inhibiting Pdx-1 expression. *Endocr Connect*, 6 (2017) 121.

39 Zhao N, Zhang A S & Enns C A, Iron regulation by hepcidin. *Journal of Clinical Investigation*, 123 (2013) 2337.

40 Rishi G, Wallace D & Subramaniam V, Hepcidin: Regulation of the master iron regulator. *Bioscience Reports*, 35 (2015) 1.

41 Li D, Jiang C, Mei G, Zhao Y, Chen L & Liu J, Quercetin Alleviates Ferroptosis of Pancreatic β Cells in Type 2 Diabetes. *Nutrients*, 12 (2020) 2954.

42 Shu T, Lv Z, Xie Y, Tang J & Mao X, Hepcidin as a key iron regulator mediates glucotoxicity-induced pancreatic beta-cell dysfunction. *Endocr Connect*, 8 (2019) 150.

43 Vodošek Hojs N, Bevc S, Ekart R & Hojs R, Oxidative Stress Markers in Chronic Kidney Disease with Emphasis on Diabetic Nephropathy. *Antioxidants (Basel)*, 9 (2020) 925.

44 Zhang YJ, Gan RY, Li S, Zhou Y & Li AN, Antioxidant Phytochemicals for the Prevention and Treatment of Chronic Diseases. *Molecules*, 20 (2015) 21138.

45 Galaris D, Barbouti A & Pantopoulos K, Iron homeostasis and oxidative stress: An intimate relationship. *Biochim Biophys Acta Mol Cell Res*, 1866 (2019) 118535.

46 Magesh S, Chen Y & Hu L, Small molecule modulators of Keap1-Nrf2-ARE pathway as potential preventive and therapeutic agents. *Med Res Rev*, 32 (2012) 687.

47 Jin T & Chen C, Umbelliferone delays the progression of diabetic nephropathy by inhibiting ferroptosis through activation of the Nrf-2/HO-1 pathway. *Food Chem Toxicol*, 163 (2022) 112892.

48 Ali RS, Lvhui S, Ni-Ya Z, Mohamed K M, Zhao L & Li C, Grape Seed Proanthocyanidin Extract Alleviates AflatoxinB-Induced Immunotoxicity and Oxidative Stress via Modulation of NF-κB and Nrf2 Signaling Pathways in Broilers. *Toxins*, 11 (2020) 1.

49 Liu P, Li J, Liu M, Zhang M, Xue Y & Zhang Y, Hesperetin modulates the Sirt1/Nrf2 signaling pathway in counteracting myocardial ischemia through suppression of oxidative stress, inflammation, and apoptosis. *Biomed Pharmacother*, 139 (2021) 111552.

50 Singh A, Venkannagari S, Oh K H, Zhang Y, Liu L & Rohde J M, Small molecule inhibitor of NRF2 selectively intervenes therapeutic resistance in KEAP1-deficient NSCLC tumors. *ACS Chem Biol*, 11 (2016) 3214.